

SWIMMING SPEED AND POWER CALCULATIONS FOR SQUIRMING CYLINDERS IN  
POROUS MEDIA

A Thesis

by

KHAI QUANG NGUYEN

BBA, Texas A&M University-Corpus Christi, 2019

Submitted in Partial Fulfillment of the Requirements for the Degree of

MASTER OF SCIENCE

in

MATHEMATICS

Texas A&M University-Corpus Christi  
Corpus Christi, Texas

May 2021

©Khai Quang Nguyen

All Rights Reserved

May 2021

SWIMMING SPEED AND POWER CALCULATIONS FOR SQUIRMING CYLINDERS IN  
POROUS MEDIA

A Thesis

by

KHAI QUANG NGUYEN

This thesis meets the standards for scope and quality of  
Texas A&M University-Corpus Christi and is hereby approved.

Devanayagam Palaniappan, PhD  
Chair

Alexey L. Sadovski, PhD  
Committee Member

M. S. Muddamallappa, PhD  
Committee Member

May 2021

## ABSTRACT

Several micro-organisms swim in heterogeneous fluid environments such as the porous media (with pores, fibers or polymers). The past decade has seen an increasing interest in understanding propulsion mechanisms of minute organisms on small scales, both theoretically and experimentally. Interest to theoretical models on locomotion strategies with homogeneous fluids in three-dimensions has a long record in applied mathematics (Lighthill, *Commun. Pure and Appl. Math.*, (1952); Blake, *J. Austr. Math. Soc.*, (1971)). In this thesis, we have studied mathematical models for the squirming motion of circular cylinders suspended in porous media governed by the two-dimensional Brinkman partial differential equations (PDE) subject to the varying surface velocity conditions on the surface of the squirmer. The vector boundary-value problem (BVP) is reduced to a scalar BVP for the fourth order PDE via Stokes stream-function formulation in polar coordinates. Exact analytical solutions for the mathematical model are found in terms of the modified Bessel functions of the integer order for various radial and tangential modes of surface oscillations. We performed the calculation of the swimming speed and power for the two-dimensional squirming motion of cylinders in heterogeneous fluids for various modes of the surface velocity changes. It is found that the non-dimensional permeability parameter, arising due to the heterogeneity of the fluid environment, has a significant impact on the velocity and pressure fields as well as the speed and power of the squirming cylinder. Our results show that the speed, which depends on the first mode only, is always less than that of the cylinder squirming in Stokes flow. The power can increase by the use of certain normalization factors. The stream-line plots reveal the existence of quadrupolar flow patterns and saddle points in the vicinity of the cylindrical squirmer. Another illustration of our method for the problem of a cylinder swimming in a homogeneous fluid (Stokes fluid) surrounded by a heterogeneous fluid (Brinkman fluid) will also be shown in this talk. We believe that the results of this thesis will be crucial in the un-

derstanding of various biological functions including bacterial movement in mucous, motility in reproduction, and escaping from predators.

## ACKNOWLEDGEMENTS

Foremost, I would like to give my sincere gratitude to my advisor, Dr. Devanayaggam Palaniappan (Dr. Pal) for giving me a chance to do the research and providing the constructive feedback on my improvement. His interest, vision, and motivation has deeply inspired me throughout my professional career. Dr. Palaniappan used his generosity with too much enthusiasm to help and guide me all the time of the research, even during the Winter break. I cannot imagine how nice he is, and not to expect to have a better advisor for my Graduate studies.

Besides that, I would like to express a special thanks to all my Committee members, Dr. Alexey Leonidovitch Sadovski and Dr. Mallikarjunaiah Muddamallappa for giving me a chance to work with, together with their encouragement and helpful comments to make the paper better.

I would like to express the appreciation to Dr. Mallikarjunaiah Muddamallappa and Dr. Beate Zimmer for teaching me the material that can be used and applied in many aspects of the research paper. Based on the high standard of the lectures, I can better understand the detail of structural motion, methodology, and mathematical operation.

In addition, I thank my classmate, Karthik Kumar Vasudeva for helping me with Latex and understanding of programming part. To my roommate, Bianca Lopez in her providing the accommodation and understanding of my story. To my best friends: David Swisher, Jerry Vo, Y Nguyen, Dung Pham, and Linh Bui in sharing the depth of my feelings when I got stress and depression.

Finally, I would like to express the deepest appreciation to all my beloved family members for providing me a good life. Thanks Mom and Dad who worked hard to afford my career and support me financially and spiritually throughout my life.

## DEDICATION

This research is dedicated to all my friends that come from Business major and cannot imagine how beautiful Math is, you may want to read it.

## TABLE OF CONTENTS

CONTENTS	PAGE
ABSTRACT . . . . .	iv
ACKNOWLEDGEMENTS . . . . .	vi
DEDICATION . . . . .	vii
TABLE OF CONTENTS . . . . .	viii
LIST OF FIGURES . . . . .	ix
CHAPTER I: INTRODUCTION . . . . .	1
CHAPTER II: MATHEMATICAL FORMULATION . . . . .	6
2.1 Darcy and Brinkman equations for the porous medium . . . . .	6
2.2 Circular Cylindrical Squirmer in Porous Medium using Brinkman Model . . . . .	7
2.3 Lighthill-Blake Type Surface Velocity Slip Boundary Conditions . . . . .	10
2.4 General Solution of the Fourth Order Equation . . . . .	11
CHAPTER III: ISOLATED CYLINDRICAL SWIMMER IN POROUS MEDIA . . . . .	13
3.1 Exact Solution for a Cylindrical Swimmer in Brinkman Medium . . . . .	14
3.2 Numerical Results . . . . .	18
CHAPTER IV: TWO-FLUID MODEL WITH SQUIRMING CYLINDER . . . . .	26
4.1 First Mode Problem . . . . .	27
4.2 Second Mode Problem . . . . .	29
CHAPTER V: SUMMARY AND CONCLUSIONS . . . . .	33
REFERENCES . . . . .	35

## LIST OF FIGURES

FIGURES	PAGE
1.1 Fluid flow in porous media (right) [30] . . . . .	3
2.2 Cylindrical squirmer in Brinkman medium . . . . .	8
3.3 The stream line for Stokes and Brinkman flow past circular cylinder in B mode at $\sigma = 0.001$ : (a-b) Pusher squirmer $\beta_2 = -0.2$ (c-d) Puller squirmer $\beta_2 = 0.2$ (e-f) Neutral squirmer $\beta_2 = 0$ . . . . .	19
3.4 The stream line for Brinkman flow past circular cylinder of pusher, puller, and neutral squirmer in B mode: (a), (d), and (g) $\sigma = 0.1$ (b), (g), and (h) $\sigma = 0.18$ (c), (f), and (i) $\sigma = 1$ . . . . .	21
3.5 Variation of Pressure versus r with various $\sigma$ at (a) $B_1 = 1, B_2 = -1$ and (b) $A_1 = 1, A_2 = -1$ . . . . .	22
3.6 Variation of Pressure versus r with various $\sigma$ at (a) $B_1 = 1, B_2 = 1$ and (b) $A_1 = 1, A_2 = 1$ . . . . .	23
3.7 Variation of Pressure versus r with various $\sigma$ at (a) $B_1 = 1, B_2 = 0$ and (b) $A_1 = 1, A_2 = 0$ . . . . .	23
3.8 Variation of swimming speed $U$ ( $A_1 = 0, B_1 = 1$ ) versus $a$ with various $\sigma$ . . . . .	24
3.9 Power P scaled by Stokes (a) puller $B_1 = 1, B_2 = 1$ and (b) neutral $B_1 = 1, B_2 = 0$ . . . . .	25
4.10 The two-fluid phase model . . . . .	27

## Nomenclature

$\mu, \mu^*$  Viscosity of the fluid and bulk viscosity of the porous, respectively

$\nabla^2$  Laplace operator

$\sigma, k$  Dimensionless parameter and permeability, respectively

$\tau_{rr}, \tau_{r\theta}$  Normal stress and shear stress on the surface of the fluid, respectively

$\vec{u}, \vec{f}$  Velocity and external force vector, respectively

$a$  Radius of cylinder

$a_n, b_n, \alpha, \beta, \gamma, \delta, \varepsilon, \xi, \kappa$  Surface coefficients

$A_n, B_n$  Radial and tangential modes in polar coordinate, respectively

$F$  Total Force

$I_0, I_1, I_2$  Modified Bessel function of the first kind of order 0, 1, 2

$K_0, K_1, K_2$  Modified Bessel function of the second kind of order 0, 1, 2

$P$  Rate of working per unit area (Power)

$p$  Pressure

$r, \theta$  Radial and angular components of polar coordinate

$U$  Swimming speed

$u, v$  Radial (normal velocity) and tangential velocity components, respectively

## CHAPTER I: INTRODUCTION

Micro-organisms of several geometrical shapes propel themselves at small length scales in heterogeneous fluid environments. The locomotion of minute organisms in a highly viscous fluid is critical in a variety of biological functions including spermatozoa reaching out to the ovum during reproduction, bacteria escaping from predators and microbes foraging for food, among many other processes [3, 9, 15]. Commonly observed microorganisms are covered with what are known as the flagella or cilia whose length scales are measured in nano meters. The beating of these flagella or cilia in coordinated fashions supply power for the microorganisms to propel in a fluid in which they perform swimming. The Reynolds number ( $Re$ ), which is the characterization of the inertial to viscous forces ratio, of the locomotion typically ranges from  $10^{-5}$  for swimming bacteria to  $10^{-4}$  for human spermatozoa [11, 14]. Specifically, the inertial effects are virtually negligible since the Reynolds number is small. The past years have seen tremendous progress in understanding the propulsion mechanisms of swimming microorganisms in various circumstances [6, 14, 25, 27] and currently, the interest in this direction is fast growing. The basic quantities that are fundamental to the knowledge of microorganism swimming phenomenon are the speed with which they propel, power and efficiency of swimming in the fluid environment. Previous studies have shown theoretical calculations of these vital physical quantities for three-dimensional problems both in homogeneous and heterogeneous fluids. While two dimensional case has been attempted for a cylindrical swimmer in a homogeneous Stokes fluid (low Reynolds number fluid) [4], the analysis for the corresponding problem in a heterogeneous media is lacking in the literature. In this thesis, we address the swimming and power calculations for a squirming cylinder in porous media.

Theoretical studies on swimming of microorganisms in inertia-less fluids evolved around calculations for spherical bodies in three dimensions (3D). Interest to mathematical models on

locomotion strategies with homogeneous fluids in 3D has a long record in applied mathematics [5, 18]. In order to improve the understanding of physical quantities associated with swimming, these studies developed the design of mobility of micro-organism (squirmer) in a viscous fluid. The squirmer is a spherical model of micro-organism swimming in a fluid in which it is suspended. It has been realized that some micro-organisms can propel themselves along with traveling wave by bending or rotating the flagella [5, 21], while other movements are generated by a beating of short cilia on their surface. The action of moving and motion (due to surface oscillations) of the micro-squirmer in a fluid is called "squirming". Particularly, Blake [5] had modeled the three-dimensional case of the dynamics of cilia propulsion based on the "envelope" that covers the cilia. His method is used on the assumption of the cilia are closed to each other and can be replaced completely by the progressive waving envelope in order to apply the no-slip conditions in symplectic metachronal wave. In the case of the certain undulations on the surface. Further, the two-dimensional self-propulsion of a circular cylinder at low Reynolds numbers was also discussed by Blake [5] using a scalar function, known as the stream function, formulation for the so called Stokes equations (equations for the low Reynolds number flow of inertial less fluid). The results of these studies have been the center of several other investigations (see for instance, [15] and references therein) of microorganism swimming in homogeneous fluids. In heterogeneous fluid environments the propulsion mechanisms are modeled by more challenging mathematical equations and therefore, the swimming characteristics can be much different.

A porous medium with a permeability parameter belongs to one of the heterogeneous fluid categories. A schematic of a porous fluid region that can be commonly seen is shown in Figure 1.1. Generally, a porous medium is defined as a physical structure containing pores (voids) with permeability, called matrix of skeletal portion and usually filled with fluid [32]. For low permeability medium with no viscous shear on the boundaries, Darcy's equation [10] has been widely employed as a model for a flow in porous medium. However, for small to relatively large

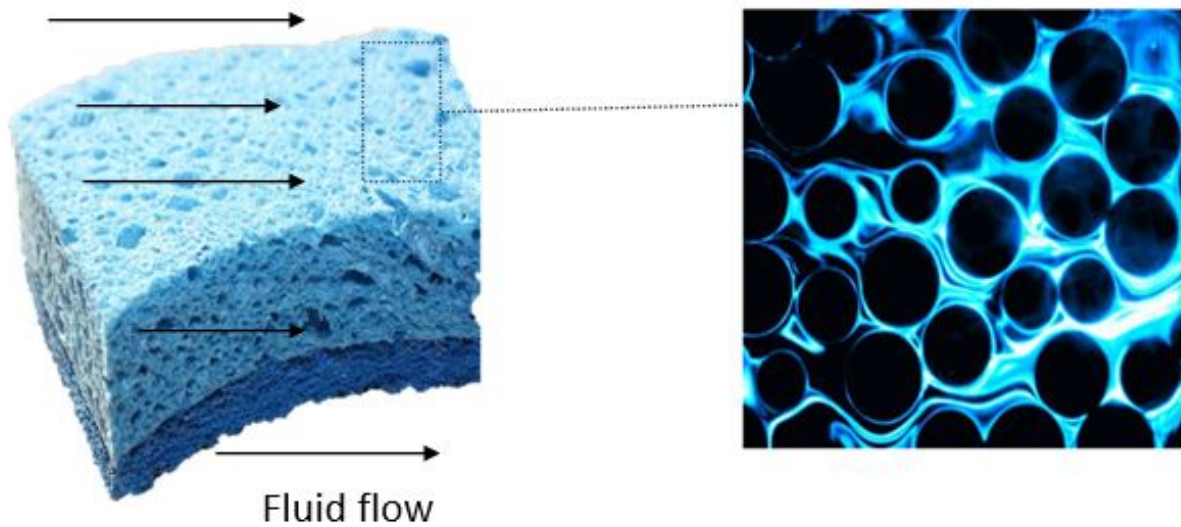


Figure 1.1  
Fluid flow in porous media (right) [30]

permeability and in the presence of viscous shear, the Darcy's equation is insufficient to describe the fluid flow. To resolve this issue, Brinkman [7] proposed a model generalizing Darcy's law that includes viscous shear. The Brinkman's model for describing the porous medium later became the generalized "Darcy-Brinkman law" and provides vector partial differential equations for the velocity and pressure fields prevailing in the heterogeneous fluid region. The presence of the permeability parameter characterises the heterogeneity of the fluid and modifies the flow profiles significantly in the presence of boundaries.

Mathematical modeling of flow past boundaries in porous media are of great interest in a wide range of other applications as well. Some of these include heat transfer analysis, chemical catalytic reactor, spread of pollutant, geothermal energy system, and oil and gas recovery [12]. The two-dimensional flow past cylindrical boundaries have also been analyzed on various occasions using homogeneous boundary conditions. For instance, Pop and Cheng [24] reported an analytical study of the incompressible flow past a cylinder in the Brinkman medium by providing the expression of the flow separation. In addition, Wang [33] has documented comparison

results for spheres and circular cylinders suspended in Brinkman fluid region using the parameter  $\sigma$  of the porous medium. Another recent study has considered the two-dimensional flow around the solid cylindrical inclusion embedded in the Brinkman porous medium with uniform velocity slip [2], that is, non-homogeneous boundary conditions. In the context of swimming, however, the squirmer problem requires the non-uniform surface variation boundary conditions. This has been successfully included for a spherical microorganism propelling in a Brinkman fluid [21] and theoretical results have been reported for the swimming velocity and the efficiency for a spherical squirmer. The results in [21] also gives a comparison of the spatial decay of flows in Brinkman model with that in a purely viscous fluid (Stokes fluid). We remark that the corresponding results for squirming motion of cylinders in porous medium have not been discussed so far in the literature.

In two-dimensional Stokes flow it is well-known that there is no solution for the uniform flow past a circular cylinder (or any other 2D body profile). This is the famous Stoke-Paradox and is in contrast to the three-dimensional case where the problem of steady uniform flow past a sphere has a unique solution. The problems of uniform flow past an obstacle in both two- and three-dimensions embedded in a Brinkman fluid have solutions and the flow past a cylinder or a sphere are readily available [7, 24, 33]. When the dimensionless permeability parameter approaches zero, the steady Brinkman flow past a sphere in a porous medium result reduces to the Stokes flow solution [33]. However, the 2D solution in porous medium does not reduce to the corresponding Stokes flow in the asymptotic limit as demonstrated recently in [19]. In fact, the expressions for the velocity gives terms that grow logarithmically far from the obstacle in the limit of vanishing permeability. Due to this undesirable situation the two-dimensional flow problems have been avoided in most of the earlier investigations. Here we show that the swimming speed and power expressions for the squirming motion of cylinders safely reproduce the required results in the limit of zero dimensionless permeability.

This thesis is organized as follows: In **Chapter 2**, we begin by introducing the Darcy-Brinkman equation and the problem of squirming motion of cylindrical micro-squirmers in the Brinkman fluid. The Lighthill-Blake type boundary conditions used on the surface of the cylinders are also discussed. In **Chapter 3**, we present derivations of analytical solutions of the fourth order PDE based on the imposing velocity slip boundary conditions. It then, in turn, allows us to calculate the velocity components in terms of various parameters. The other physical quantities such as stress on the surface, force, swimming speed, and the rate of working per unit area (power) for a squirming cylinder in porous media are also determined. In **Chapter 4**, we analyse the two-fluid phase model (Stokes-Brinkman fluids). We state the problem of a squirming cylinder in a viscous fluid (Stokes fluid) surrounded by a porous medium modeled by Brinkman equations. The appropriate boundary conditions for the two-fluid model are stated as well. We also derive analytic solutions for a squirming cylinder in a viscous fluid enclosed by the Brinkman medium. Various limiting cases of our results from the exact solutions presented here are also given in this chapter. Finally, in **Chapter 5**, we document our key findings of the work reported in this thesis.

The symbols in this paper are taken from the references and are listed in the Nomenclature. The format of the thesis is followed by the standard format of the TAMUCC template.

## CHAPTER II: MATHEMATICAL FORMULATION

Better understanding of the squirming motion of objects in a fluid medium requires the knowledge of analytical and numerical solutions of mathematical equations modeling the physical problem. The fluid in our current investigation is treated as a porous medium which is a material volume consisting of a solid matrix with interconnected voids. The ratio of void space to the total volume of the medium is defined as the permeability of the porous medium [7, 10]. Depending on the low and high permeability (or porosity) situations the porous media equations can be stated as demonstrated by Darcy and Brinkman in their study. In this chapter, we provide the two formulations for the porous medium in two-dimensions leading to the first and second order vector partial differential equations proposed by Darcy [10] and Brinkman [7]. We then formulate the problem of a squirming cylinder in a porous medium using the two-dimensional stream function formulation. We also state the surface velocity boundary conditions similar to those proposed by Lighthill [18] and Blake [5] for a spherical squirmer in Stokes flow. This completes the statement of the physical problem of a cylindrical squirmer in Brinkman fluid in two-dimensions. We close this section by giving a brief derivation of the general solution of the scalar fourth order partial differential equation satisfied by the Stokes stream function for its use in subsequent sections.

### 2.1 Darcy and Brinkman equations for the porous medium

The model for the fluid flow in the porous media was initially investigated by Henry Darcy (1856). He pointed out the relationship between the instantaneous discharge rate, the viscosity of the fluid, and the pressure drop over the distance [10] and is famously known as Darcy law. It actually relates the flow velocity to the pressure gradient in a linear fashion across the porous

medium. The Darcy's law in mathematical form can be written as

$$\vec{\mathbf{u}} = -\frac{\mu}{k}\nabla p + \vec{\mathbf{f}}, \quad (2.1)$$

$$\nabla \cdot \vec{\mathbf{u}} = 0. \quad (2.2)$$

In the above equations  $\vec{\mathbf{u}}$  represents the filtration velocity,  $p$  is the pressure,  $k$  is permeability of the porous medium,  $\mu$  is the viscosity of the fluid and  $\vec{\mathbf{f}}$  is the external force. Note that the second equation is the mass balance or the incompressibility condition. The Darcy's equations predict the flow behavior when the permeability and pressure gradients are sufficiently small. For large values of  $k$ , Darcy law becomes inadequate due to the absence of viscous stronger effects as pointed out later by Brinkman [7]. Indeed, Brinkman [7, 8] proposed a modified set of equations that generalizes Darcy's law including the viscous forces on the boundaries. Brinkman equations can be cast in the form

$$\nabla^2 \vec{\mathbf{u}} - \frac{\mu^*}{\mu k} \vec{\mathbf{u}} = \frac{1}{\mu} \nabla p + \vec{\mathbf{f}}, \quad (2.3)$$

$$\nabla \cdot \vec{\mathbf{u}} = 0, \quad (2.4)$$

where  $\mu^*$  is the bulk viscosity. The above set of Brinkman equations or the generalized Darcy-Brinkman equations are found to be more suitable for several flow problems in porous media [16, 24] as well as squirming motions [17, 21] and provide more accurate results. Therefore, we use Brinkman equations in our model to represent the flow in porous medium. In the following section, we provide the mathematical setting stating the governing equations and the relevant boundary conditions for a cylindrical squirmer problem in a porous medium.

## 2.2 Circular Cylindrical Squirmer in Porous Medium using Brinkman Model

Consider an infinitely long two-dimensional cylindrical squirmer of radius  $a$  immersed in a porous medium. We choose  $(x, y)$  as the coordinate axes in a two-dimensional Cartesian frame,

and let  $(r, \theta)$  represent the corresponding polar coordinates (see Figure 2.2). The surface of the squirmer is given by  $r = a$ . Let  $\vec{u} = (u, v)$  be the velocity of the fluid at any point, where  $u(r, \theta)$  and  $v(r, \theta)$  are the components of  $\vec{u}$  in the radial and tangential directions, respectively. As noted in the previous sub-section, for relatively large permeability values, Brinkman equations are more appropriate describing the flow in a porous media. The justification of the use of Brinkman equations to model porous media has also been evident in many studies [19, 21, 24, 33]. Therefore, in our model, we utilize the two-dimensional Brinkman equations for the flow of fluid in the porous medium. The momentum and mass balance equations of the Brinkman equations in

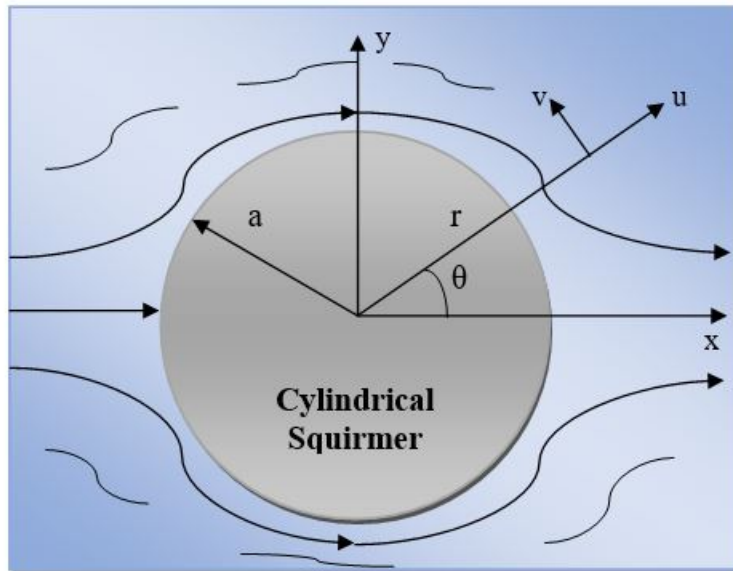


Figure 2.2  
Cylindrical squirmer in Brinkman medium

two dimensions in the absence of external forces can be written in the vector form as (see the

subsection 2.1)

$$\mu(\nabla^2 \vec{\mathbf{u}} - \frac{\mu^*}{\mu k} \vec{\mathbf{u}}) = \nabla p, \quad (2.5)$$

$$\nabla \cdot \vec{\mathbf{u}} = 0, \quad (2.6)$$

where the Laplace operator in polar coordinates is defined as

$$\nabla^2 \equiv \frac{\partial^2}{\partial r^2} + \frac{1}{r} \frac{\partial}{\partial r} + \frac{1}{r^2} \frac{\partial^2}{\partial \theta^2}. \quad (2.7)$$

The component form of vector equation (2.5) and (2.6) are

$$\left( \frac{\partial^2 u}{\partial r^2} + \frac{1}{r} \frac{\partial u}{\partial r} + \frac{1}{r^2} \frac{\partial^2 u}{\partial \theta^2} - \frac{u}{r^2} - \frac{2}{r^2} \frac{\partial v}{\partial \theta} \right) - \frac{\mu^*}{\mu k} u = \frac{1}{\mu} \frac{\partial p}{\partial r}, \quad (2.8)$$

$$\left( \frac{\partial^2 v}{\partial r^2} + \frac{1}{r} \frac{\partial v}{\partial r} + \frac{1}{r^2} \frac{\partial^2 v}{\partial \theta^2} - \frac{v}{r^2} + \frac{2}{r^2} \frac{\partial u}{\partial \theta} \right) - \frac{\mu^*}{\mu k} v = \frac{1}{\mu r} \frac{\partial p}{\partial \theta}, \quad (2.9)$$

$$\frac{\partial}{\partial r}(ru) + \frac{\partial v}{\partial \theta} = 0. \quad (2.10)$$

The continuity equation (2.10) implies the existence of the scalar function  $\psi(r, \theta)$ . The velocity components  $u$  and  $v$  in term of  $\psi(r, \theta)$  becomes:

$$u = \frac{1}{r} \frac{\partial \psi}{\partial \theta} \quad v = -\frac{\partial \psi}{\partial r} \quad (2.11)$$

Elimination of pressure between (2.8) and (2.9) by cross differentiation and using (2.10) above, we can reduce the system in the form

$$\nabla^2(\nabla^2 - \sigma^2)\psi = 0 \quad (2.12)$$

where  $\sigma^2 = \frac{\mu^*}{\mu k}$  represents a dimensionless permeability parameter. Thus, the vector equations (2.5) - (2.6) for the velocity and pressure fields reduce to solving the scalar equation (2.12) for the stream function. In the next subsection, we discuss the appropriate boundary conditions on the cylindrical squirmer and formulate the Boundary Value Problem (BVP) in a Brinkman medium.

### 2.3 Lighthill-Blake Type Surface Velocity Slip Boundary Conditions

The squirmer problem under investigation requires a set of appropriate boundary conditions, in addition to the governing equation of motion (discussed in the preceding subsection). In the case of three-dimensional Stokes flow, the commonly used boundary conditions are those proposed by Lighthill and used by Blake for a spherical squirmer. In fact, Lighthill [18] in 1952 first introduced a model for the squirming motion of a nearly spherical body in a viscous fluid in the zero Reynolds number limit. He discussed the mechanism of propulsion by investigating the small oscillation on the shape. Blake [5] later developed the model of self-propulsion due to the oscillation on the surface of the spherical squirmer using his spherical envelope approach. These conditions have been extensively used in several settings [14, 15, 21, 22]. The corresponding two-dimensional problem was also discussed by Blake [4] for a cylindrical geometry in Stokes flow. In this thesis, we plan to use the conditions adopted by Blake [4] in our model consisting of a cylindrical squirmer in Brinkman medium. On the oscillating surface of the cylindrical case in two-dimensions, Blake used the following set of boundary conditions on the cylinder surface ( $r = a$ ):

$$u(a, \theta) = \sum_{n=0}^{\infty} A_n \cos(n\theta) \qquad v(a, \theta) = \sum_{n=1}^{\infty} B_n \sin(n\theta) \qquad (2.13)$$

The constants  $A_n$  and  $B_n$  are the radial and tangential modes of the velocity variations on the cylindrical surface, respectively. The above conditions allow the surface velocity slip variations (variable slip velocity) across the surface of the cylindrical swimmer. In our analysis we use the boundary conditions given in (2.13) to solve the squirming problem in porous media. Note that the above boundary conditions imply that the tangential velocity has to be an odd function in  $\theta$ , that is  $v(r, \theta) = -v(r, -\theta)$ . This then allows the streaming flow past the cylinder that can occur giving a finite stream at infinity, unlike the Stokes paradox. In other words, this assumption correctly predicts that there is no solution of Stokes equations that satisfies the no-slip condition

[5] and producing finite velocity at infinity. Although this paradoxical behavior does not exist in Brinkman flows [2, 19], we point out that one needs to be cautious while performing the zero parameter limit calculations to test for the Stokes flow results. Equations (2.12) and (2.13) provides the required boundary value problem (BVP) for the squirming motion of a cylinder in porous media modeled by Brinkman equations.

#### 2.4 General Solution of the Fourth Order Equation

For a later use, we provide here a brief derivation of the solution of the fourth order scalar equation (2.12) for the stream function. First, we set  $\nabla^2 \psi = \Upsilon$ . Then (2.12) becomes

$$(\nabla^2 - \sigma^2)\Upsilon = 0 \quad (2.14)$$

Following the separation of variables method for PDE, we let  $\Upsilon = R(r)\Theta(\theta)$  where  $R, \Theta \neq 0$ . Note that  $\Upsilon(r, \theta)$  need to be  $2\pi$  periodic in  $\theta$  [20]. With this substitution the separable form of (2.14) become

$$\frac{r^2 R''}{R} + \frac{rR'}{R} - \sigma^2 r^2 = -\frac{\Theta''}{\Theta} = \lambda \quad (2.15)$$

Now the separated equations are

$$r^2 R'' + rR' - (\sigma^2 r^2 + \lambda)r = 0, \quad (2.16)$$

$$\Theta'' + \lambda \Theta = 0. \quad (2.17)$$

Using the periodic Boundary Condition  $\Theta(2\pi) = \Theta(0)$  and for the eigenvalues  $\lambda > 0$ , the nontrivial solution of (2.17) is

$$\Theta_n(\theta) = A_n \cos(n\theta) + B_n \sin(n\theta) \quad (2.18)$$

Similarly, equation (2.16) has its solution in terms of the modified Bessel functions of the first and second kind  $I_n(\sigma r)$  and  $K_n(\sigma r)$ , respectively. The resulting solution reads

$$R_n(r) = C_n I_n(\sigma r) + D_n K_n(\sigma r) \quad (2.19)$$

Then the product solution of  $\Upsilon$  in eigen-function form is

$$\Upsilon(r, \theta) = \sum_{n=0}^{\infty} (C_n I_n(\sigma r) + D_n K_n(\sigma r)) (A_n \cos(n\theta) + B_n \sin(n\theta)). \quad (2.20)$$

Since  $\nabla^2 \psi = \Upsilon$  is a non-homogeneous PDE, we need to find two solutions, viz., homogeneous and particular solutions. For the homogeneous part, we let  $\psi = F(r)\Theta(\theta)$  where  $F, \Theta \neq 0$ . Due to the  $2\pi$  periodic condition, the equation  $\nabla^2 \psi = 0$  yields

$$\frac{r^2 F''}{F} + \frac{r F'}{F} = -\frac{\Theta''}{\Theta} = \lambda \quad (2.21)$$

Equation (2.21) can be rewritten in the form

$$r^2 F'' + r F' - \lambda F = 0 \quad (2.22)$$

$$\Theta'' + \lambda \Theta = 0 \quad (2.23)$$

Adopting a similar approach used to solve (2.16) then (2.17), the equation (2.22) yields the Euler system written as  $F_n(r) = C_n r^n + D_n r^{-n}$  when  $n \geq 1$  and  $C_0 + D_0 \ln(r)$  when  $n = 0$ . Then the general solution of the homogeneous solution for  $\nabla^2 \psi = 0$  is

$$\psi_c(r, \theta) = C_0 + D_0 \ln(r) + \sum_{n=1}^{\infty} (C_n r^n + D_n r^{-n}) (A_n \cos(n\theta) + B_n \sin(n\theta)) \quad (2.24)$$

The particular solution is [20]

$$\psi_p(r, \theta) = \frac{1}{\sigma^2} \sum_{n=1}^{\infty} (C_n I_n(\sigma r) - D_n K_n(\sigma r)) (A_n \cos(n\theta) + B_n \sin(n\theta)) \quad (2.25)$$

Then the general solution of the inhomogeneous PDE (2.12) is  $\psi(r, \theta) = \psi_c + \psi_p$ . The complete solution can be represented in the form [33]

$$\begin{aligned} \psi(r, \theta) = & C_0 + D_0 \ln(r) + \sum_{n=1}^{\infty} (C_n r^n + D_n r^{-n}) (A_n \cos(n\theta) + B_n \sin(n\theta)) \\ & + \frac{1}{\sigma^2} \sum_{n=1}^{\infty} (E_n I_n(\sigma r) - F_n K_n(\sigma r)) (A_n \cos(n\theta) + B_n \sin(n\theta)) \end{aligned} \quad (2.26)$$

As pointed out earlier, this solution is obtained by the method of separation of variables for linear PDEs. In the next chapters, we use this general form to obtain analytical solutions of the stream function(s) for the cylindrical squirmer problems in porous media.

### CHAPTER III: ISOLATED CYLINDRICAL SWIMMER IN POROUS MEDIA

The scalar stream function formulation of the cylindrical squirmer problem stated in (2.12) subject to the slip velocity conditions (2.13) will now be used to generate analytical solutions for a cylindrical swimmer in a Brinkman fluid. Determination of the stream function provides a basis for the discussion of the flow fields prevailing in the presence of a squirmer. By a direct differentiation process, one can obtain the required velocity components via the relations given in (2.11). These essential quantities are required for the swimming speed and power calculations of the squirming cylinder in porous media modeled by Brinkman equations in two dimensions. Of course, the pressure can be obtained by a direct integration using (2.8) and (2.9). The steps involved in the calculation of speed and power due to the squirming motion of a cylinder in Brinkman medium are given below.

- Use the general solution of (2.12) for the stream function with arbitrary constants
- Apply the surface velocity boundary conditions (2.13) to determine the arbitrary constants in the stream function for various radial and tangential modes
- Find velocity components via direct differentiation using (2.11)
- Compute pressure and stress components
- Integrate stresses to find a force on the cylinder
- Use force-free condition to obtain the swimming speed [4, 21]
- Determine the power using integration of the product of velocity and stress components on the surface of the squirmer

Below we use the aforementioned steps to determine the relevant physical quantities of interest in the context of squirming motion of a circular cylinder.

### 3.1 Exact Solution for a Cylindrical Swimmer in Brinkman Medium

We consider the uniform flow of an incompressible viscous fluid along the  $y$ -direction with  $\psi_0(r, \theta) = -Ur \sin \theta$  [4]. The speed  $U$  is unknown and can be calculated for a squirmer suspended in the fluid. Now in the presence of a cylindrical squirmer we take the solution in the form (see (2.26))

$$\psi(r, \theta) = a_0 \theta - Ur \sin(\theta) + \sum_{n=1}^{\infty} \left[ \frac{a_n}{r^n} + b_n K_n(\sigma r) \right] \sin(n\theta). \quad (3.27)$$

where  $a_0$ ,  $a_n$  and  $b_n$  are the constants to be determined. In (3.27), the conditions of finite velocities at infinity (far away from the cylinder) is incorporated. Note that each term in the summation is a solution of (2.12) due to the linearity of the Brinkman equations. For  $n = 1, 2$ , the stream functions extracted from (3.27) are given by

$$\psi_1 = \left[ -Ur + \frac{a_1}{r} + b_1 K_1(\sigma r) \right] \sin(\theta) \quad (3.28)$$

$$\psi_2 = \left[ \frac{a_2}{r^2} + b_2 K_2(\sigma r) \right] \sin(2\theta) \quad (3.29)$$

Applying the surface velocity conditions (2.13), and using (3.27) and (2.11), we obtain a system of algebraic equations for the unknown coefficients from which one can determine

$$a_0 = A_0 a \quad (3.30)$$

$$a_1 = \left[ A_1 + U - \frac{K_1(\sigma a)}{a} b_1 \right] a^2 \quad b_1 = \frac{B_1 - A_1 - 2U}{\sigma K_0(\sigma a)} \quad (3.31)$$

$$a_n = \frac{a^{n+1}}{n} A_n - a^n K_n(\sigma a) b_n \quad b_n = \frac{B_n - A_n}{\sigma K_{n-1}(\sigma a)} \quad (3.32)$$

Now the velocity components can be obtained by the use of (2.11) as

$$u(r, \theta) = \frac{a_0}{r} - U \cos(\theta) + \sum_{n=1}^{\infty} \left[ \frac{n}{r^{n+1}} a_n + \frac{n K_n(\sigma r)}{r} b_n \right] \cos(n\theta) \quad (3.33)$$

$$v(r, \theta) = U \sin(\theta) + \sum_{n=1}^{\infty} \left[ \frac{n}{r^{n+1}} a_n + \left( \sigma K_{n-1}(\sigma r) + \frac{n K_n(\sigma r)}{r} \right) b_n \right] \sin(n\theta) \quad (3.34)$$

Using (3.30) - (3.32), the above equations take the form

$$u = \frac{A_0 a}{r} + U \left[ \frac{a^2}{r^2} - 1 - 2H_1 \right] \cos(\theta) + \sum_{n=1}^{\infty} \left[ \left( \frac{a^{n+1}}{r^{n+1}} - H_n \right) A_n + H_n B_n \right] \cos(n\theta) \quad (3.35)$$

$$v = U \left( \frac{a^2}{r^2} + 1 - 2G_1 \right) \sin(\theta) + \sum_{n=1}^{\infty} \left[ \left( \frac{a^{n+1}}{r^{n+1}} - G_n \right) A_n + G_n B_n \right] \sin(n\theta) \quad (3.36)$$

where

$$H_n = \frac{n}{r} \left( \frac{K_n(\sigma r) - a^n r^{-n} K_n(\sigma a)}{\sigma K_{n-1}(\sigma a)} \right) \quad G_n = \left( H_n + \frac{K_{n-1}(\sigma r)}{K_{n-1}(\sigma a)} \right) \quad (3.37)$$

Note:

$$\frac{K_n(\sigma r) - a^n r^{-n} K_n(\sigma a)}{\sigma K_{n-1}(\sigma a)} \cong \frac{a^{n+1} - a^{n-1} r^2}{2r^n} + Error \quad (3.38)$$

$$\frac{K_{n-1}(\sigma r)}{K_{n-1}(\sigma a)} \cong \frac{a^{n-1}}{r^{n-1}} + Error \quad (3.39)$$

We note that expressions (3.35) - (3.37) provide the velocity fields for a cylindrical squirmer in a Brinkman fluid. In the limit  $\sigma \rightarrow 0$  these results produce logarithmic terms [19], as in Stokes paradox. However, the solution forms for the velocity fields in (3.35) - (3.37) are similar to those given by Blake [4] for a cylindrical squirmer in two-dimensional Stokes flow.

The pressure can be obtained by substituting (3.35) - (3.37) into (2.8) and (2.9). After some algebra, one finds

$$p = \mu \sigma^2 \left[ -a A_0 \ln(r) + U r \cos(\theta) + \sum_{n=1}^{\infty} \frac{a_n}{r^n} \cos(n\theta) \right]. \quad (3.40)$$

This completes the four steps in our procedure to determine swimming speed and power calculations. Next we proceed to compute the stress components using

$$\tau_{rr} = p - 2\mu \frac{\partial u}{\partial r} \quad (3.41)$$

$$\tau_{r\theta} = -\mu \left[ r \frac{\partial}{\partial r} \left( \frac{v}{r} \right) + \frac{1}{r} \frac{\partial u}{\partial \theta} \right]. \quad (3.42)$$

Substitution of (3.35), (3.36), and (3.40) in (3.41) and (3.42) yields

$$\begin{aligned} \tau_{rr} = \mu \left\{ \left( -\sigma^2 \ln(r) + \frac{2}{r^2} \right) a_0 + \sigma^2 U r \cos(\theta) \right. \\ \left. + \sum_{n=1}^{\infty} \left[ \left( \frac{\sigma^2}{r^n} + \frac{2n(n+1)}{r^{n+2}} \right) a_n + \left( 2\sigma n \frac{K_{n-1}(\sigma r)}{r} + 2n(n+1) \frac{K_n(\sigma r)}{r^2} \right) b_n \right] \cos(n\theta) \right\} \quad (3.43) \end{aligned}$$

$$\begin{aligned} \tau_{r\theta} = \mu \sum_{n=1}^{\infty} \left[ \frac{2n(n+1)}{r^{n+2}} a_n \right. \\ \left. + \left( (3\sigma - \sigma n) \frac{K_{n-1}(\sigma r)}{r} + \sigma^2 K_n(\sigma r) + (n^2 + n + 2) \frac{K_n(\sigma r)}{r^2} \right) b_n \right] \sin(n\theta) \quad (3.44) \end{aligned}$$

Inserting the constants from (3.30) - (3.32) results in

$$\begin{aligned} \tau_{rr} = \mu \left\{ \left( \frac{2}{a} - \sigma^2 a \ln(a) \right) A_0 + 2 \left( \sigma^2 a + \frac{\sigma K_1(\sigma a)}{K_0(\sigma a)} \right) U \cos(\theta) \right. \\ \left. + \sum_{n=1}^{\infty} \left[ \left( \frac{\sigma^2 a}{n} + \frac{\sigma K_n(\sigma a)}{K_{n-1}(\sigma a)} + \frac{2}{a} \right) A_n + \left( \frac{2n}{a} - \frac{\sigma K_n(\sigma a)}{K_{n-1}(\sigma a)} \right) B_n \right] \cos(n\theta) \right\} \quad (3.45) \end{aligned}$$

$$\begin{aligned} \tau_{r\theta} = \mu \left\{ -\frac{2\sigma K_1(\sigma a)}{K_0(\sigma a)} U \sin(\theta) \right. \\ \left. + \sum_{n=1}^{\infty} \left[ \left( \frac{2n}{a} - \frac{\sigma K_n(\sigma a)}{K_{n-1}(\sigma a)} \right) A_n + \left( \frac{2}{a} + \frac{\sigma K_n(\sigma a)}{K_{n-1}(\sigma a)} \right) B_n \right] \sin(n\theta) \right\} \quad (3.46) \end{aligned}$$

The crucial step now is to find the force acting on the cylinder which is calculated from [4]

$$F = \int_0^{2\pi} a [\tau_{rr} \cos(\theta) - \tau_{r\theta} \sin(\theta)]_{r=a} d\theta \quad (3.47)$$

Using (3.45) and (3.46), the force on the cylinder, after integration using orthogonality conditions  $\forall m, n > 0$ :

$$\int_0^{2\pi} \sin(m\theta) \sin(n\theta) d\theta = \begin{cases} 0, & m \neq n \\ \pi, & m = n \end{cases} \quad (3.48)$$

and similarly,

$$\int_0^{2\pi} \cos(m\theta) \cos(n\theta) d\theta = \begin{cases} 0, & m \neq n \\ \pi, & m = n \end{cases} \quad (3.49)$$

(3.47) becomes

$$F = \mu\pi \left[ (\sigma a)^2 (A_1 + 2U) - 2a(B_1 - A_1 - 2U) \frac{\sigma K_1(\sigma a)}{K_0(\sigma a)} \right] \quad (3.50)$$

If we let  $A_1 = B_1 = 0$ , the equation (3.50) agrees with those given in [31, 33] for the force acting on a no-slip cylinder in Brinkman fluid. Utilizing the force-free condition for a squirmer [4, 21] the swimming/propulsion speed  $U$  is determined to be

$$U = \frac{1}{2}(B_1 - A_1) - \frac{(\sigma a)B_1}{2 \left[ (\sigma a) + 2 \frac{K_1(\sigma a)}{K_0(\sigma a)} \right]}. \quad (3.51)$$

Note that the swimming speed depends only on the first radial and tangential modes ( $A_1$  and  $B_1$ ) as in three-dimensional Brinkman flow [21]. The first term in (3.51) is the swimming speed of a cylinder in Stokes flow [4] and the second term is the fluid resistance due to the parameter  $\sigma$ . It is interesting that this last term in (3.51) does not contain  $A_1$  for a squirmering cylinder in Brinkman medium where as the swimming speed in 3D is affected by the radial mode associated with the permeability [21]. It can be seen from (3.50) that the denominator in the second term of (3.51) is the same as the normalizing factor appearing in the expression for the force with  $A_1 = B_1 = 0$ . This result may have a significant physical meaning in the context of swimming. Further, it can be seen from (3.51) that the speed in Brinkman flow is less than that in Stokes flow for  $B_1 > 0$ .

In Stokes flow, the swimming speed does not change whether a stationary cylinder is placed in a uniform flow or the cylinder is moving in stationary fluid. This is because the pressure gradient at infinity is the zero in both cases. In Brinkman flow, the pressure gradient in the uniform flow is zero. But a moving object induces a pressure gradient far away from the boundary. This in turn produces a difference in the hydrodynamic drag/force as noted in [13]. A similar observation

can be made for the squirming cylinder in porous media. If the squirmer moves in a stationary Brinkman fluid then the swimming speed, denoted by  $U^*$ , can be calculated in the same way and is given by

$$U^* = \frac{1}{2}(B_1 - A_1) - \frac{(\sigma a)(B_1 + A_1)}{2 \left[ (\sigma a) + 4 \frac{K_1(\sigma a)}{K_0(\sigma a)} \right]} \quad (3.52)$$

Notice the appearance of the  $A_1$  mode in the second term in the above equation due to the non-zero pressure gradient.

Finally, the power  $P$  can be determined using [4]

$$P = \frac{1}{2\pi} \int_0^{2\pi} (u\tau_{rr} + v\tau_{r\theta})_{r=a} d\theta. \quad (3.53)$$

Substituting (3.35) - (3.37), (3.41) and (3.42) in (3.53) and after integrating one obtains

$$P = \frac{\mu}{2} \left\{ 2 \left( \sigma^2 a A_1 + (A_1 - B_1) \frac{\sigma K_1(\sigma a)}{K_0(\sigma a)} \right) U + \sum_{n=1}^{\infty} \left[ \frac{\sigma^2 a}{n} A_n^2 + \left( \frac{2}{a} + \frac{\sigma K_n(\sigma a)}{K_{n-1}(\sigma a)} \right) (A_n^2 + B_n^2) + 2 \left( \frac{2n}{a} - \frac{\sigma K_n(\sigma a)}{K_{n-1}(\sigma a)} \right) A_n B_n \right] \right\}. \quad (3.54)$$

This last concluding step completes the speed and power calculations for a cylindrical swimmer in porous media modeled by Brinkman equations.

### 3.2 Numerical Results

Let us now turn our attention on the numerical results extracted from the analytical solutions for the squirming problem of a cylinder derived in the preceding subsection. The parameters such as the radial and tangential mode amplitudes  $A_n$ ,  $B_n$ , and parameter  $\sigma$  can influence the velocity field, pressure, swimming speed and power. Therefore, we choose these parameters and analyze variations. In the following we record our findings based on the graphical illustrations produced using the analytic expressions presented in the subsection 3.1.

#### Streamline Topology

### STOKES - BRINKMAN

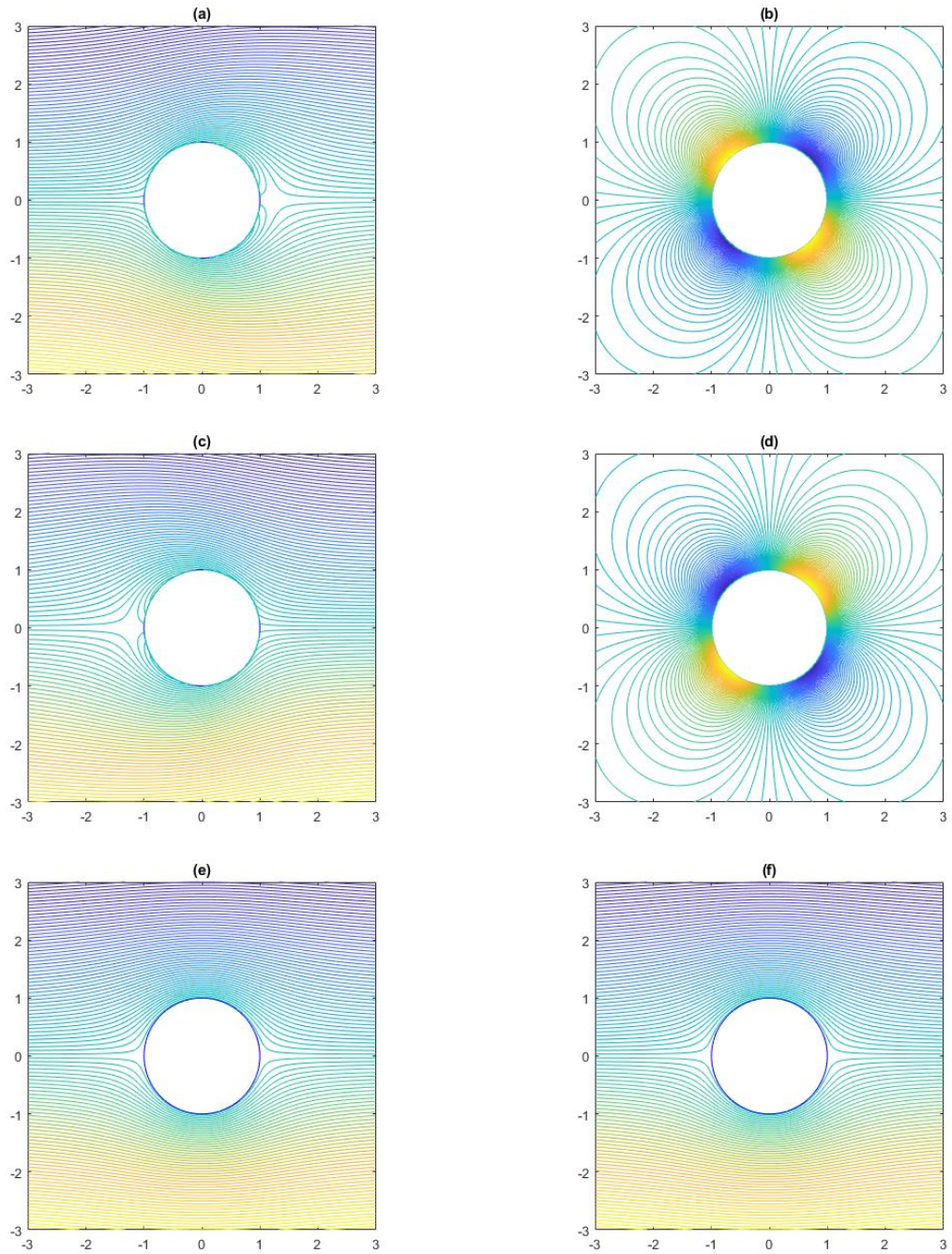


Figure 3.3  
The stream line for Stokes and Brinkman flow past circular cylinder in B mode at  $\sigma = 0.001$ :  
(a-b) Pusher squirmer  $\beta_2 = -0.2$  (c-d) Puller squirmer  $\beta_2 = 0.2$  (e-f) Neutral squirmer  $\beta_2 = 0$

First, the streamlines for the first two modes are plotted in Figure 3.3 using the stream functions given in (3.28) and (3.29). Note that we have defined the parameter  $\beta_2 = \frac{B_2}{B_1}$  that characterizes different types of motion [21]. In the context of swimming,  $\beta_2 < 0$  is a pusher,  $\beta_2 > 0$  is a puller and  $\beta_2 = 0$  is a neutral swimmer. For the sake of simplicity we consider the tangential modes in the streamline plots. Figure 3.3 portrays the streamline topology for Stokes (a), (c), (e) and Brinkman flows (b), (d), (f). The value of the parameter  $\sigma$  is taken to be small ( $\sigma = 0.001$ ) for the sake of comparison. In the case of Stokes flow, the presence of cylindrical swimmer induces a saddle point close to the cylinder wall for the pusher. Its location is opposite for the puller as can be seen in Figure 3.3 (a) and (c). But in Brinkman flow, quadrupolar flow lines appear for pusher and puller and the pattern is distinct from that in Stokes flow (see Figure 3.3 (b), (d)). It appears that the modified Bessel functions cause such flow patterns in the case of squirming cylinder in porous media. For the neutral swimmer, however, the flow patterns are very similar in Stokes and Brinkman flows as in Figure 3.3 (e), (f). We have tested the streamline patterns for various other values of  $\sigma$  and observed that flow topology can be quite different than shown here. The streamline patterns for a squirming cylinder in Brinkman fluid for three parameter values,  $\sigma = 0.1$ ,  $\sigma = 0.18$  and  $\sigma = 1$ , are displayed in Figure 3.4. For pusher the quadrupolar lines start to appear when  $\sigma = 0.1$  as observed in Figure 3.4 (a). Increase in the value of  $\sigma$  changes the quadrupolar patterns significantly and further increase in  $\sigma$  completely nullifies such patterns as evident from figure 3.4 (b), (c). A triplet of saddle points start appearing in the flow region as seen in Figure 3.4 (c). Higher values of parameter may be considered depending on the practicality of the squirmer model. We remark that such flow patterns are due to the permeability of the porous medium. A similar trend can be seen for the puller (see Figure 3.4 (d), (e), (f)), but the flow direction is opposite to that of the pusher. For the neutral swimmer, the streamlines do not seem to be affected by the increase of  $\sigma$  as shown in Figure 3.4 (i), (j), (k). Flow lines can be drawn by considering radial modes as well in a similar fashion.

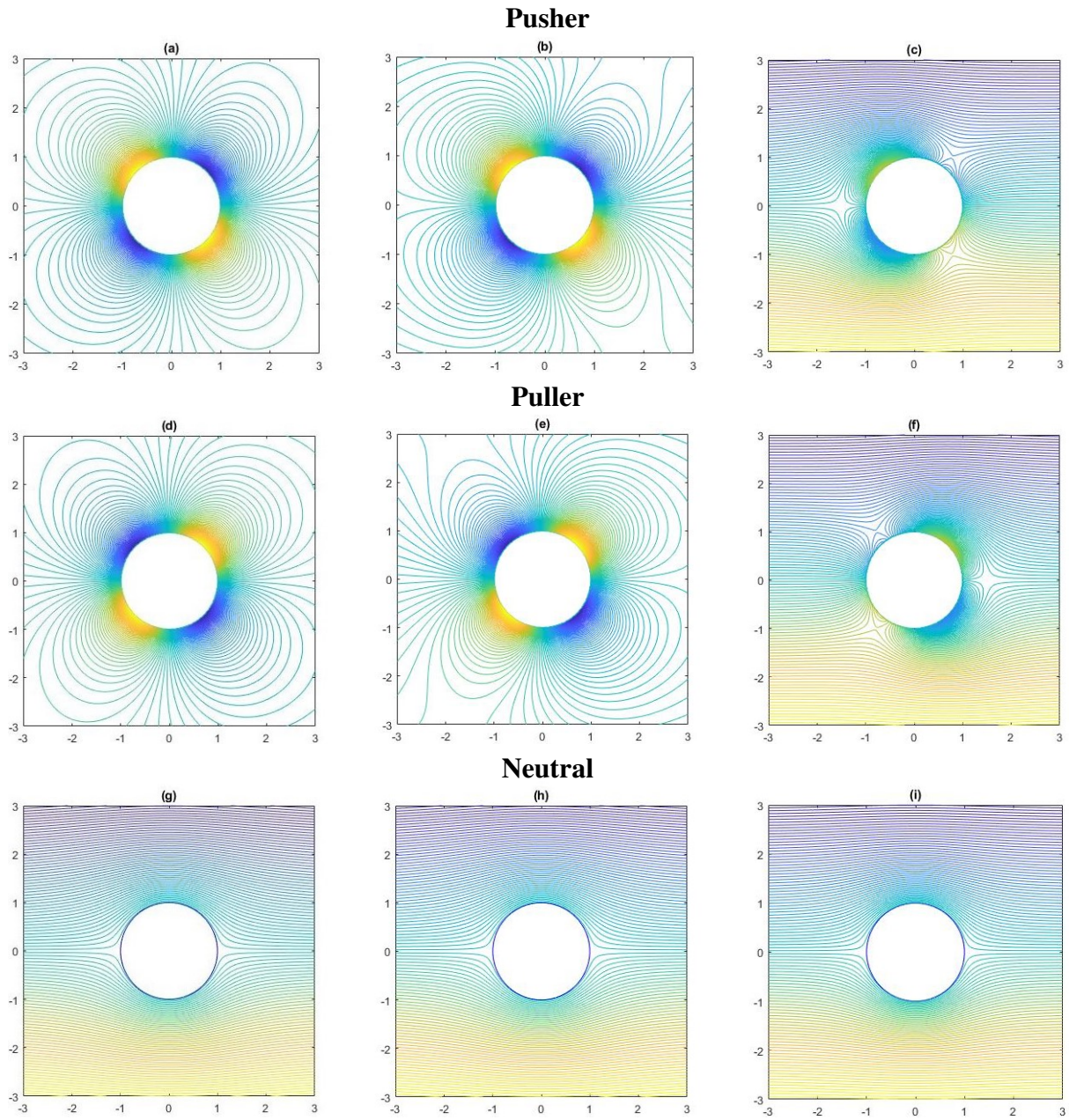


Figure 3.4  
 The stream line for Brinkman flow past circular cylinder of pusher, puller, and neutral squirmer in B mode: (a), (d), and (g)  $\sigma = 0.1$  (b), (e), and (h)  $\sigma = 0.18$  (c), (f), and (i)  $\sigma = 1$

## Pressure Variations

The graphical illustration of the pressure versus the radial coordinate  $r$ , plotted using (3.40), for pusher is shown in Figure 3.5. Here we consider both radial and tangential modes separately. As shown in Figure 3.5 (a), the pressure first decreases for all values of  $\sigma$  until a minimum value is reached and then increases with  $r$  in the presence of tangential modes ( $B_1 = 1$  and  $B_2 = -1$ ). It is also noted that the pressure decreases with the increase in the permeability. With radial modes (see Figure 3.5 (b)), the behavior of pressure appears to be reversed. It increases first (up to a maximum value) and then decreases for  $A_1 = 1$  and  $A_2 = -1$ . For the puller, the pressure increases for the tangential modes until reaching a maximum value for each  $\sigma$  and then becomes a constant. For small values of the permeability, pressure increases much faster as in Figure 3.6 (a). Gain the behavior is reversed in the case of radial modes (see Figure 3.6 (b)). Finally, for the neutral swimmer  $\beta_2 = 0$ , the pressure increases linearly for tangential modes and decreases (linearly) for the radial modes as seen from Figure 3.7 (a), (b).

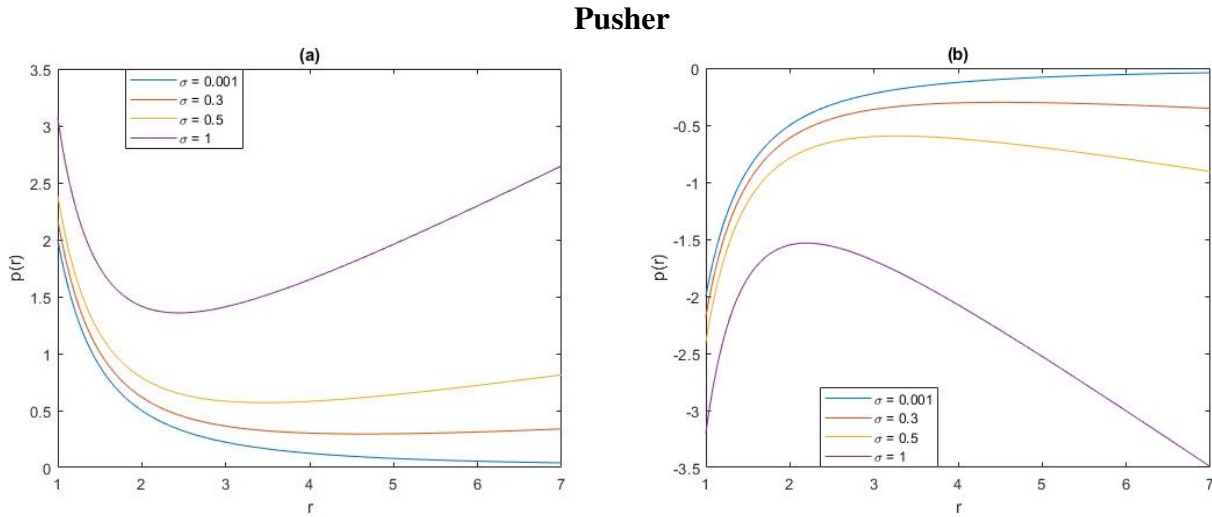


Figure 3.5  
Variation of Pressure versus  $r$  with various  $\sigma$  at (a)  $B_1 = 1, B_2 = -1$  and (b)  $A_1 = 1, A_2 = -1$

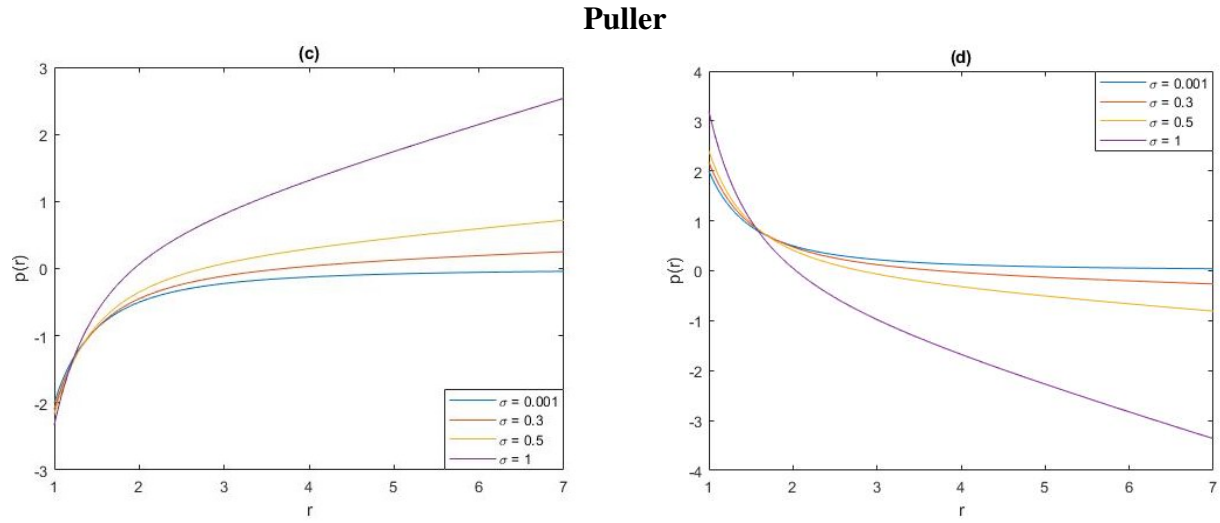


Figure 3.6  
 Variation of Pressure versus  $r$  with various  $\sigma$  at (a)  $B_1 = 1, B_2 = 1$  and (b)  $A_1 = 1, A_2 = 1$

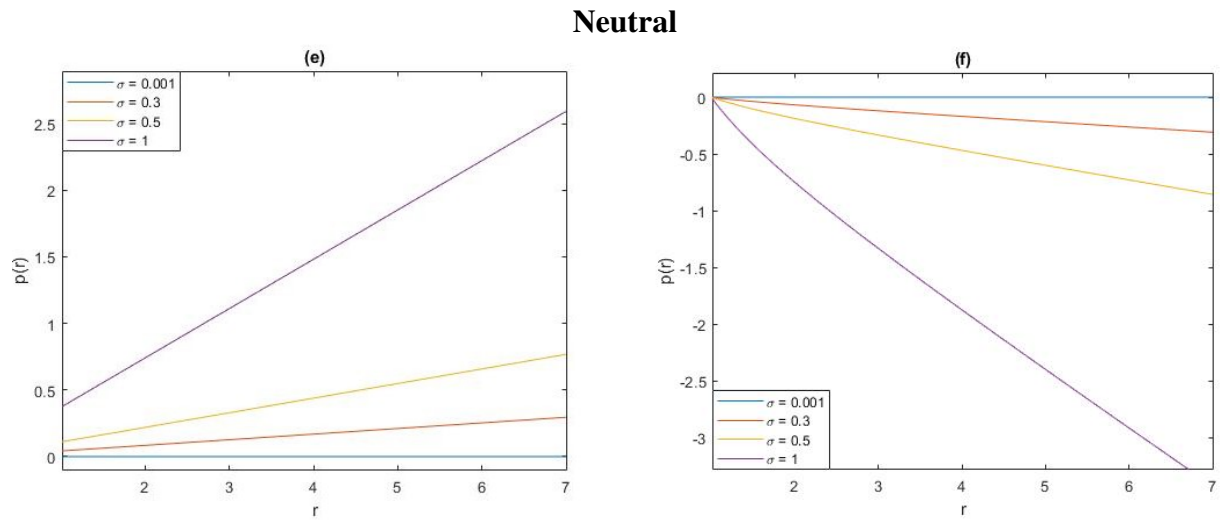


Figure 3.7  
 Variation of Pressure versus  $r$  with various  $\sigma$  at (a)  $B_1 = 1, B_2 = 0$  and (b)  $A_1 = 1, A_2 = 0$

### Swimming Speed

The variation of the swimming speed of a cylindrical squirmer in Brinkman fluid is shown in Figure 3.8. The plots are drawn using the expression given in (3.51) for various  $\sigma$ . It is

observed that the speed in Brinkman fluid is always less than that of the squirmer in Stokes flow. Further, the speed decreases with the radius of the squirmer and becomes almost zero for larger values of  $a$ . This implies that the presence of permeability of the porous medium slows down the swimming speed in Brinkman flows. It can be shown that using the asymptotic limit in (3.51) our results can be reduced to those in Stokes flow.

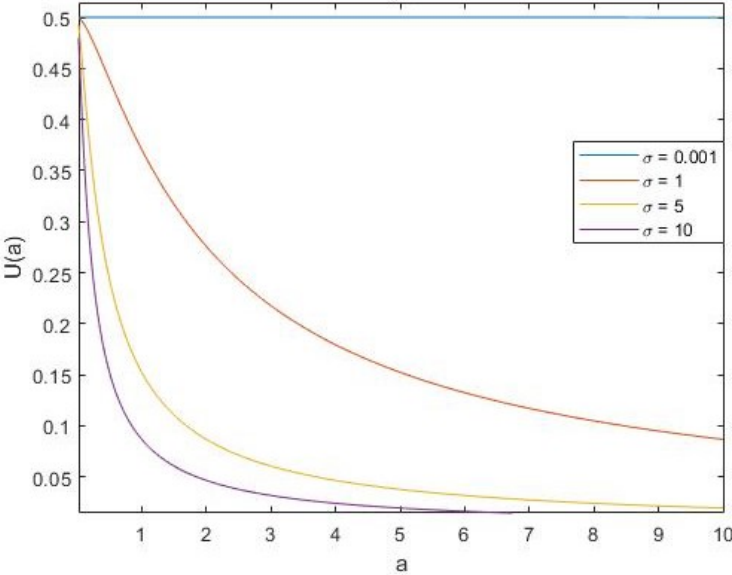


Figure 3.8  
Variation of swimming speed  $U$  ( $A_1 = 0, B_1 = 1$ ) versus  $a$  with various  $\sigma$

## Power

The expression for power is given in (3.54) for all modes. The result for two modes can be extracted from the general expression for the power. The extracted result is scaled by the power in Stokes flow (with  $B_1$  and  $B_2$  modes, see [4]) which is  $P_S = \frac{\mu}{a}(B_1^2 + B_2^2)$ . The plots of the scaled power  $\frac{P}{P_S}$  versus parameter  $\sigma$  are shown in Figure 3.9 for puller and neutral cases. It is clear that the scaled quantity (power) increases with increasing  $\sigma$  in both cases. For pusher, we have observed a similar variation with the parameter. The presented results may be of interest in modeling cylindrical squirmer in porous medium.

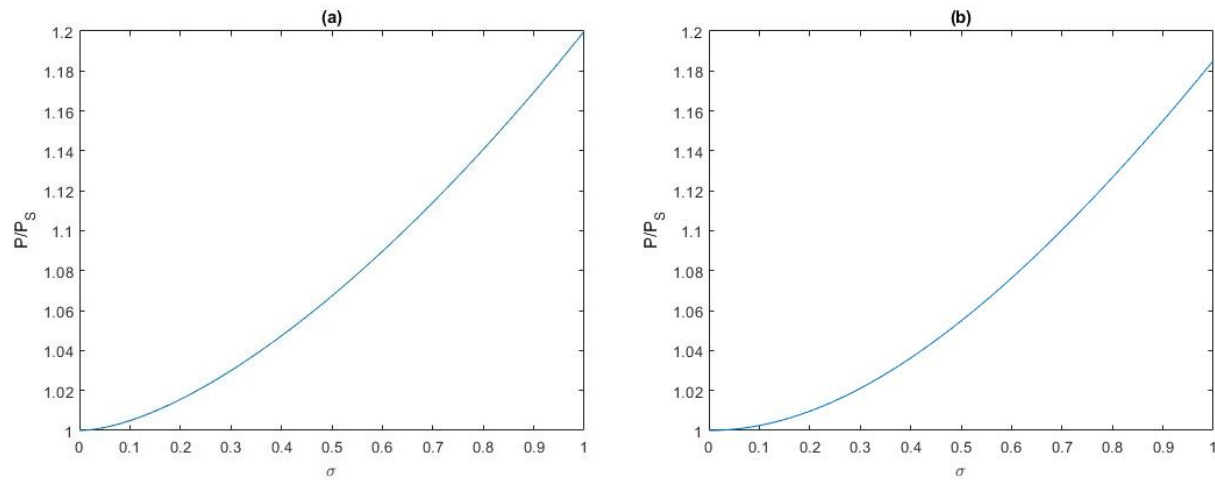


Figure 3.9  
Power  $P$  scaled by Stokes (a) puller  $B_1 = 1, B_2 = 1$  and (b) neutral  $B_1 = 1, B_2 = 0$

## CHAPTER IV: TWO-FLUID MODEL WITH SQUIRMING CYLINDER

In this chapter we present mathematical results for a squirmer in a viscous fluid enclosed by a porous medium. Similar problems in three dimensions for spherical squirmers have been discussed in [23, 26]. The geometry of this two-fluid model is depicted in Figure 4.10. We consider a cylindrical squirmer of radius  $a$  placed in Stokes fluid which is surrounded by the Brinkman fluid. The boundary between the two fluids is also circular and has the radius  $b \geq a$  as shown in Figure 4.10. The model equations in the Stokes and Brinkman flow regions as in [23] are as follows:

Stokes region:

$$\mu \nabla^2 \vec{\mathbf{u}}_S = \nabla p_S, \quad (4.55)$$

$$\nabla \cdot \vec{\mathbf{u}}_S = 0. \quad (4.56)$$

Brinkman region:

$$\mu \nabla^2 \vec{\mathbf{u}}_B - \sigma^2 p_B = 0, \quad (4.57)$$

$$\nabla \cdot \vec{\mathbf{u}}_B = 0. \quad (4.58)$$

We use the general solution of the Stokes equations in 2D given in [4] and (2.26) in chapter II for the Brinkman medium to derive analytic solutions for one and two modes. The boundary conditions on the squirmer  $r = a$  and on the outer boundary  $r = b$  are assumed as follows.

- On  $r = a$ , use surface velocity conditions given in (2.13). These are the usual conditions for a cylindrical squirmer
- On  $r = b$ , apply the continuity of two velocities and stresses.

The BVP for this problem will have more constants to be determined using the above boundary conditions. The solution procedure is similar to that used for a cylindrical swimmer in

Brinkman fluid demonstrated in Chapter III. Below we discuss the first and second mode problems separately.

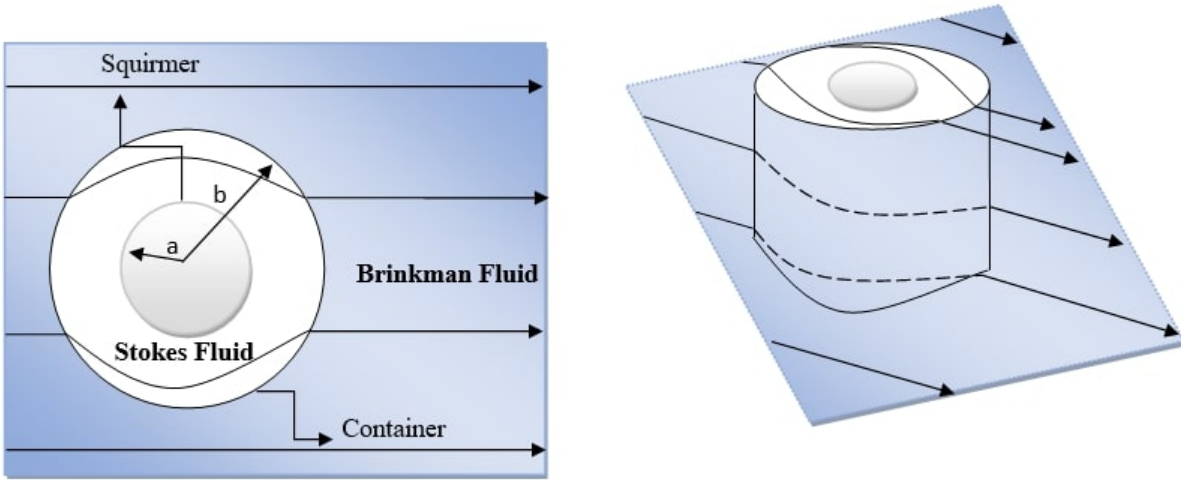


Figure 4.10  
The two-fluid phase model

#### 4.1 First Mode Problem

For the one mode problem the stream functions in the Stokes and Brinkman flow regions are taken in the form

$$\psi_S(r, \theta) = -Ur \sin(\theta) + a_0 \theta + \frac{a_1}{r} \sin(\theta) + \alpha_1 r \sin(\theta) + \beta_1 r^3 \sin(\theta) \quad (4.59)$$

$$\psi_B(r, \theta) = \frac{\gamma_1}{r} \sin(\theta) + \delta_1 K_1(\sigma r) \sin(\theta) \quad (4.60)$$

The boundary conditions become:

On  $r = a$ , using (2.13) we must have

$$u(a, \theta) = A_0 + A_1 \cos(\theta) \quad v(a, \theta) = B_1 \sin(\theta) \quad (4.61)$$

On  $r = b$  the boundary conditions using the continuity of velocity and stress components can be written as

$$\begin{cases} u_S = u_B, & v_S = v_B \\ \tau_{Srr} = \tau_{Brr}, & \tau_{Sr\theta} = \tau_{Br\theta} \end{cases} \quad (4.62)$$

The velocity components, using (2.11) in the Stokes and Brinkman regions become

$$\begin{cases} u_S = \frac{a_0}{r} + \left[ -U + \frac{a_1}{r^2} + \alpha_1 + \beta_1 r^2 \right] \cos(\theta) \\ u_B = \left[ \frac{\gamma_1}{r^2} + \frac{K_1(\sigma r)}{r} \delta_1 \right] \sin(\theta) \end{cases} \quad (4.63)$$

and

$$\begin{cases} v_S = \left[ U + \frac{a_1}{r^2} - \alpha_1 - 3\beta_1 r^2 \right] \sin(\theta) \\ v_B = \left[ \frac{\gamma_1}{r^2} + \left( \sigma K_0(\sigma r) + \frac{K_1(\sigma r)}{r} \right) \delta_1 \right] \sin(\theta) \end{cases} \quad (4.64)$$

The pressure for Stokes - Brinkman region are given by

$$p_S = 8\mu\beta_1 r \cos(\theta) \quad p_B = \mu \frac{\sigma^2}{r} \gamma_1 \cos(\theta) \quad (4.65)$$

From equation (3.41) - (3.42), we calculate the stress components in the two regions which are given by

$$\begin{cases} \tau_{Srr} = \mu \left[ \frac{2}{r^2} a_0 + \left( 4r\beta_1 + \frac{4}{r^3} a_1 \right) \cos(\theta) \right] \\ \tau_{Brr} = \mu \left[ \left( \frac{\sigma^2}{r} + \frac{4}{r^3} \right) \gamma_1 + \left( 2\sigma \frac{K_0(\sigma r)}{r} + 4 \frac{K_1(\sigma r)}{r^2} \right) \delta_1 \right] \cos(\theta) \end{cases} \quad (4.66)$$

and

$$\begin{cases} \tau_{Sr\theta} = \mu \left( \frac{4}{r^3} a_1 + 4r\beta_1 \right) \sin(\theta) \\ \tau_{Br\theta} = \mu \left[ \frac{4}{r^3} \gamma_1 + \left( \sigma^2 K_1(\sigma r) + 2\sigma \frac{K_0(\sigma r)}{r} + 4 \frac{K_1(\sigma r)}{r^2} \right) \delta_1 \right] \sin(\theta) \end{cases} \quad (4.67)$$

Using the boundary conditions (4.61) and (4.62) above, we form a system of 5 equations involving 5 unknowns. Solving the resulting system of algebraic equations yields the coefficients as follows:

$$a_0 = 0 \quad (4.68)$$

$$a_1 = (A_1 + B_1) \frac{a^2}{2} + a^4 \beta_1 \quad (4.69)$$

$$\delta_1 = \frac{B_1 - A_1}{\sigma K_0(\sigma b)} + \frac{4b^2(\delta^2 - 1)}{\sigma K_0(\sigma b)} \beta_1 \quad (4.70)$$

$$\gamma_1 = \frac{b(B_1 - A_1)K_1(\sigma b)}{\sigma K_0(\sigma b)} + \frac{4b^3(\delta^2 - 1)K_1(\sigma b)}{\sigma K_0(\sigma b)} \beta_1 \quad (4.71)$$

$$\alpha_1 = \frac{A_1 - B_1}{2} + U - 2a^2 \beta_1 \quad (4.72)$$

where

$$\beta_1 = \frac{(B_1 - A_1)\sigma K_1(\sigma b)}{8bK_0(\sigma b) - 4\sigma b^2(\delta^2 - 1)K_1(\sigma b)}, \quad \delta = \frac{a}{b}. \quad (4.73)$$

Imposing  $\alpha_1 = 0$  (the force-free condition), we obtain the swimming speed  $U$  of the cylindrical squirmer using the two-fluid model as:

$$U = 2a^2 \beta_1 + \frac{(B_1 - A_1)}{2} \quad (4.74)$$

The Power is then calculated, using (3.53), in the form

$$P_{1S} = 4\mu \left( \frac{a_1}{a^3} + \beta_1 a \right) \left( \frac{a_1}{a^2} - a^2 \beta_1 \right). \quad (4.75)$$

In the limit  $\sigma \rightarrow 0$ ,  $\beta_1 \rightarrow 0$  the swimming speed reduces to  $U_S$  which is  $\frac{1}{2}(B_1 - A_1)$ . The same procedure for power as  $a = b$  gives

$$P_S = \frac{\mu}{a} (A_1 + B_1)^2, \quad (4.76)$$

which is the result for a cylinder in Stokes flow [4].

## 4.2 Second Mode Problem

Following the same approach as in the first mode problem and applying the relevant boundary conditions we can derive analytic solutions for the two-mode problem. The stream functions in the two fluid phases are

$$\psi_S(r, \theta) = \frac{a_2}{r^2} \sin(2\theta) + \alpha_2 r^2 \sin(2\theta) + \varepsilon_2 r^4 \sin(2\theta) + \kappa_2 \sin(2\theta) \quad (4.77)$$

$$\psi_B(r, \theta) = \frac{\gamma_2}{r^2} \sin(2\theta) + \delta_2 K_2(\sigma r) \sin(2\theta) \quad (4.78)$$

The boundary conditions are now the following.

On  $r = a$ , using equation (2.13)

$$u(a, \theta) = A_2 \cos(2\theta) \quad v(a, \theta) = B_2 \sin(2\theta) \quad (4.79)$$

On  $r = b$ , using the continuity of velocity and stresses conditions

$$\begin{cases} u_S = u_B, & v_S = v_B \\ \tau_{Srr} = \tau_{Brr}, & \tau_{Sr\theta} = \tau_{Br\theta} \end{cases} \quad (4.80)$$

Using (2.11), the velocity components of the Stokes and Brinkman regions are

$$\begin{cases} u_S = \left[ \frac{2a_2}{r^3} + 2r\alpha_2 + 2r^3\epsilon_2 + \frac{2\kappa_2}{r} \right] \cos(2\theta) \\ u_B = \left[ \frac{2\gamma_2}{r^3} + \frac{2K_2(\sigma r)}{r} \delta_2 \right] \sin(2\theta) \end{cases} \quad (4.81)$$

and

$$\begin{cases} v_S = \left[ \frac{2a_2}{r^3} - 2r\alpha_2 - 4r^3\epsilon_2 \right] \sin(2\theta) \\ v_B = \left[ \frac{2\gamma_2}{r^3} + \left( \sigma K_1(\sigma r) + \frac{2K_2(\sigma r)}{r} \right) \delta_2 \right] \sin(2\theta) \end{cases} \quad (4.82)$$

The pressure in the respective regions become

$$p_S = \mu \left( 12\epsilon_2 r^2 + \frac{4\kappa_2}{r^2} \right) \cos(2\theta) \quad p_B = \mu \frac{\sigma^2}{r^2} \gamma_2 \cos(2\theta) \quad (4.83)$$

From (3.41) and (3.42), the stress components are found to be

$$\begin{cases} \tau_{Srr} = \mu \left[ \frac{12a_2}{r^4} - 4\alpha_2 + \frac{8\kappa_2}{r^2} \right] \cos(2\theta) \\ \tau_{Brr} = \mu \left[ \left( \frac{\sigma^2}{r^2} + \frac{12}{r^4} \right) \gamma_2 + \left( 4\sigma \frac{K_1(\sigma r)}{r} + 12 \frac{K_2(\sigma r)}{r^2} \right) \delta_2 \right] \cos(2\theta) \end{cases} \quad (4.84)$$

and

$$\begin{cases} \tau_{Sr\theta} = \mu \left( \frac{12}{r^4} a_2 + 4\alpha_2 + 12r^2\epsilon_2 + \frac{4\kappa_2}{r^2} \right) \sin(2\theta) \\ \tau_{Br\theta} = \mu \left[ \frac{12}{r^4} \gamma_2 + \left( 2\sigma \frac{K_1(\sigma r)}{r} + \sigma^2 K_2(\sigma r) + 12 \frac{K_2(\sigma r)}{r^2} \right) \delta_2 \right] \sin(2\theta) \end{cases} \quad (4.85)$$

The 6 constants are determined using the boundary conditions and are given by

$$a_2 = \frac{a^3}{2}B_2 + a^4\alpha_2 + 2a^6\varepsilon_2 \quad (4.86)$$

$$\delta_2 = \frac{(B_2 - A_2)\delta}{\sigma K_1(\sigma b)} + \frac{4b(\delta^2 - 1)}{\sigma K_1(\sigma b)}\alpha_2 + \frac{6b^3(\delta^4 - 1)}{\sigma K_1(\sigma b)}\varepsilon_2 \quad (4.87)$$

$$\gamma_2 = \left[ \frac{(A_2 - B_2)(4aK_1(\sigma b) - \sigma abK_2(\sigma b))}{\sigma^2 K_1(\sigma b)} \right] + \left[ \frac{-16a^2 K_1(\sigma b) + 4\sigma b^3(\delta^2 - 1)K_2(\sigma b)}{\sigma^2 K_1(\sigma b)} \right] \alpha_2 \\ + \left[ \frac{-24a^4 K_1(\sigma b) + 6\sigma b^5(\delta^4 - 1)K_2(\sigma b)}{\sigma^2 K_1(\sigma b)} \right] \varepsilon_2 \quad (4.88)$$

$$\kappa_2 = \left( \frac{A_2 - B_2}{2} \right) a - 2a^2\alpha_2 - 3a^4\varepsilon_2 \quad (4.89)$$

where

$$\alpha_2 = \left[ \frac{(A_2 - B_2)(2aK_1(\sigma b) - \sigma abK_2(\sigma b))}{8a^2 K_1(\sigma b) - 4\sigma b^3(\delta^2 - 1)K_2(\sigma b)} \right] - \left[ \frac{6b^4(\delta^4 + 1)K_1(\sigma b) - 3\sigma b^5(\delta^4 - 1)K_2(\sigma b)}{4a^2 K_1(\sigma b) - 2\sigma b^3(\delta^2 - 1)K_2(\sigma b)} \right] \varepsilon_2 \quad (4.90)$$

and

$$\varepsilon_2 = \frac{(\Pi_1 - 2\Pi_2)K_1(\sigma b) + (\sigma b^2\Pi_2)K_2(\sigma b)}{(\Pi_3 - 2\Pi_4 - 96b^5)K_1(\sigma b) + (\sigma b\Pi_4)K_2(\sigma b)} \quad (4.91)$$

where

$$\Pi_1 = -2\sigma^2 ab^3 A_2 \quad (4.92)$$

$$\Pi_2 = 12\sigma^5 a^4 b^4 B_2 (A_2 - B_2) (\delta^2 - 1) (\delta^4 - 1) \quad (4.93)$$

$$\Pi_3 = (\delta^2 - 1) (8\sigma^2 b^7 - 24\sigma^2 a^2 b^5) \quad (4.94)$$

$$\Pi_4 = b(\delta^2 - 1) [\sigma^2 b^6 (\delta^6 - 1) + 3\sigma^2 a^2 b^4 (\delta^2 - 1) + 48b^4] \quad (4.95)$$

The swimming speed does not depend on the second mode. The power obtained using (3.53)

is

$$P_{2S} = 8\mu \left[ \frac{3a_2^2}{a^7} + \frac{3a_2\kappa_2}{a^5} + \frac{\kappa_2^2}{a^3} - \alpha_2^2 a - 3\alpha_2\varepsilon_2 a^3 - 3\varepsilon_2^2 a^5 \right] \quad (4.96)$$

For small argument of the Bessel functions  $\sigma \rightarrow 0$ , the above result reduces to the one given by Blake [4] which reads

$$P_S = \frac{\mu}{a} [2(A_2^2 + B_2^2) + 2A_2B_2]. \quad (4.97)$$

For general modes the calculations can be repeated by using the same approach as above.

## CHAPTER V: SUMMARY AND CONCLUSIONS

The squirring motion of a circular cylinder in porous media modeled by the Brinkman equations is addressed in this thesis. Exact analytical solutions for a cylindrical squirmer embedded in Brinkman fluid are obtained by solving the fourth order boundary value problem for the stream function. The closed form analytic solutions are then used to calculate the swimming speed and power due to the squirring cylinder. It is found that the dimensionless parameter  $\sigma$  significantly affects the physical quantities in the model. Specifically, the following conclusions are drawn from our mathematical analysis of the squirring cylinder problem.

- Dimensionless parameter  $\sigma$  induces quadrupolar streamline patterns in the flow. Saddle points exist in the vicinity of the cylindrical squirmer for larger permeability.
- The pressure for the pusher ( $\beta_2 < 0$ ) and puller ( $\beta_2 > 0$ ) have maximum and minimum values for various permeability values of the porous medium. For the neutral swimmer ( $\beta_2 = 0$ ), the pressure is a linear increasing or decreasing function. Here  $\beta_2 = \frac{B_2}{B_1}$ , is the ratio of the first and second modes of oscillation induced via boundary conditions.
- The swimming speed  $U$  is always less than that of a cylindrical swimmer in Stokes flow. In fact, it is found to decrease for increasing values of  $\sigma$ .
- The power due to the squirring motion of the cylinder increases or decreases based on the normalizing factor. For a specific normalization, the power could be an increasing function of  $\sigma$ .
- $\sigma \rightarrow 0$  limit yields results for a squirring cylinder in Stokes flow, but the velocities contain logarithmic functions that do not become finite at infinity [19].

Our results for a squirming problem are compact and can be implemented in practice quite easily. In order to demonstrate the efficacy of our approach, we solved a two-fluid model for the squirming of a cylinder in a viscous fluid surrounded by the outside Brinkman medium. The calculations yielded closed form solutions involving the first and second modes of surface oscillation. The calculated swimming speed and power correctly reproduces the corresponding results in Stokes flows. Derivation of solutions, speed and power calculations can be done in similar fashion explained in this thesis. We believe that our results can be utilized for a better understanding of various swimming mechanisms in porous media.

## REFERENCES

- [1] Abramowitz, M. Stegun, I. A. and Romer, R. H. Handbook of mathematical functions with formulas, graphs, and mathematical tables. *American Association of Physics Teachers*, 1988.
- [2] Alshehri, N. Mathematical results for slipping flows past a cylinder or a sphere embedded in a porous medium. *Tamucc Thesis Dissertation*, 2015.
- [3] Blair, D. F. Membrane Topology of the MotA Protein of Escherichia coil. *Journal of molecular biology*, 251(2): 237–242, 1995.
- [4] Blake, J. R. Self propulsion due to oscillations on the surface of a cylinder at low Reynolds number. *Bulletin of the Australian Mathematical Society*, 5(2): 255–264, 1971.
- [5] Blake, J. R. A spherical envelope approach to ciliary propulsion. *Journal of Fluid Mechanics*, 46(1): 199–208, 1971.
- [6] Brennen, C. and Winet, H. *Annu. Rev. Fluid Mech*, 1977.
- [7] Brinkman, H. C. A calculation of the viscous force exerted by a flowing fluid on a dense swarm of particles. *Flow, Turbulence and Combustion*, 1(1): 27–34, 1949.
- [8] Brinkman, H. C. On the permeability of media consisting of closely packed porous particles. *Flow, Turbulence and Combustion*, 1(1): 81–86, 1949.
- [9] Chen, Y. Lordi, N. Taylor, M. and Pak, O. S. Helical locomotion in a porous medium. *Physical Review E*, 102(4), 043111, 2020.
- [10] Darcy, H. Les fontaines publiques de la ville de Dijon. *Victor Dalmont*, 1856.
- [11] Fauci, L. J. and Dillon, R. Biofluidmechanics of reproduction. *Annu. Rev. Fluid Mech*, 38: 371–394, 2006.

- [12] Happel, J. and Brenner, H. Low Reynolds number hydrodynamics: with special applications to particulate media. 1, 2012. Springer Science & Business Media.
- [13] Howells, I. D. Drag due to the motion of a Newtonian fluid through a sparse random array of small fixed rigid objects. *Journal of Fluid Mechanics*, 64(3): 449–476, 1974.
- [14] Lauga, E. and Powers, T. R. The hydrodynamics of swimming microorganisms. *Reports on Progress in Physics*, 72(9), 096601, 2009.
- [15] Lauga, E. Bacterial hydrodynamics. *Annual Review of Fluid Mechanics*, 48: 105–130, 2016.
- [16] Leont'ev, N. E. Flow past a cylinder and a sphere in a porous medium within the framework of the Brinkman equation with the Navier boundary condition. *Fluid Dynamics*, 49(2): 232–237, 2014.
- [17] Leshansky, A. M. Enhanced low-Reynolds-number propulsion in heterogeneous viscous environments. *Physical Review E*, 80(5), 051911, 2009.
- [18] Lighthill, M. J. On the squirming motion of nearly spherical deformable bodies through liquids at very small Reynolds numbers. *Communications on Pure and Applied Mathematics*, 5(2): 109–118, 1952.
- [19] Martin, P. A. Two-dimensional Brinkman flows and their relation to analogous Stokes flows. *IMA Journal of Applied Mathematics*, 84(5): 912–929, 2019.
- [20] Myint-U, T and Lokenath, D. Linear Partial Differential Equations for Scientists and Engineers. *Springer Science & Business Media*, 2007.
- [21] Nganguia, H. and Pak, O. S. Squirming motion in a Brinkman medium. *Journal of Fluid Mechanics*, 855: 554–573, 2018.
- [22] Nganguia, H. Zhu, L. Palaniappan, D. and Pak, O. S. Squirming in a viscous fluid enclosed by a Brinkman medium. *Physical Review E*, 101(6), 2020.
- [23] Palaniappan, D. On some general solutions of transient Stokes and Brinkman equations. *Journal of Theoretical and Applied Mechanics*, 52, 2014.

- [24] Pop, I. and Cheng, P. Flow past a circular cylinder embedded in a porous medium based on the Brinkman model. *International Journal of Engineering Science*, 30(2): 257–262, 1992.
- [25] Purcell, E. M. and Morgan, R. A. PHYS847 Quantitative Biology Reading List. *Am J Phys*, 45, 3–11, 1977.
- [26] Reigh, S. Y. and Lauga, E. Two-fluid model for locomotion under self-confinement. *Physical Review Fluids*, 2(9), 093101, 2017.
- [27] Sitti, M. Voyage of the microrobots. *Nature*, 458(7242), 1121-1122, 2009.
- [28] Smith, S. H. Slow oscillatory Stokes flow. *Quarterly of Applied Mathematics*, 55(1): 1–22, 1997.
- [29] Sondak, D. Hawley, C. Heng, S. Vinsonhaler, R. Lauga, E. and Thiffeault, J. L. Can phoretic particles swim in two dimensions?. *Physical Review E*, 94(6), 062606, 2016.
- [30] Souzy, M. Lhuissier, H. Méheust, Y. Le Borgne, T. and Metzger, B. Velocity distributions, dispersion and stretching in three-dimensional porous media. *Journal of Fluid Mechanics*, 891, 2020.
- [31] Spielman, L. and Goren, S. L. Model for predicting pressure drop and filtration efficiency in fibrous media. *Environmental Science and Technology*, 2(4): 279-287, 1968.
- [32] Su, B. Sanchez, C. and Yang, X. Y. Hierarchically structured porous materials: from nanoscience to catalysis, separation, optics, energy, and life science. *John Wiley and Sons*, 2012.
- [33] Wang, C. Y. Darcy-Brinkman flow with solid inclusions. *Chemical Engineering Communications*, 197(3): 261–274, 2009.